Geomechanics and Engineering, Vol. 2, No. 4 (2010) 303-319
DOI: http://dx.doi.org/10.12989/gae.2010.2.4.303

Effect of grain crushing on 1D compression and 1D creep behavior of sand at high stresses

Z. Wang[1] and R.C.K. Wong*[2]

[1]*Geotechnical and Structural Engineering Research Center, Shandong University, Jinan, Shandong, China, 250061*
[2]*Department of Civil Engineering, Schulich School of Engineering, The University of Calgary, 2500 University Drive NW, Calgary, Alberta, Canada T2N 1N4*

(Received March 10, 2010, Accepted September 29, 2010)

Abstract. The effect of grain crushing on the deformation of sand in 1D compression and 1D creep at high stresses was investigated theoretically and experimentally. An approach was proposed to formulate the process of grain crushing in sand in accordance with the laws of fracture mechanics and energy conservation. With this approach, the relation between the void ratio and the amount of grains crushed in 1D compression was derived. Laboratory test data were used to verify this derived relation. In addition, it was observed that there are similarities in evolution of grain size distribution in 1D compression and 1D creep tests. This implies that the changes in microstructure in sand under 1D compression and 1D creep are comparable.

Keywords: sand; grain crushing; grain size evolution; creep; compression; fracture mechanics.

1. Introduction

In general, the deformation of sandy soil is induced microscopically by contact deformation, grain sliding and rolling, and grain crushing. The contributions of these deformation modes are different at different stress levels (Mitchell and Soga 2005). At very low stress level, the contact deformation dominates the deformation of the soil. The soil behaves elastically and the deformation is reversible. Grain sliding and rolling dominate the deformation of the soil at low stress level, while grain crushing dominates the deformation of the soil at high stress level. In the latter two conditions, most of the deformation is irreversible.

The geotechnical properties of granular soil at high stresses depend on the integrity of the grains or the amount of grains crushed in soil (Lade *et al.* 1996). For instance, it is widely accepted that the 1D compression of sand at high stress levels and its yielding are closely related to grain crushing (Roberts and De Souza 1958, Coop 1990, Hagerty *et al.* 1993, Nakata *et al.* 1999, Nakata *et al.* 2001, Graham *et al.* 2004, Wood 2007, Mesri and Vardhanabhuti 2009). The yield stress of granular soil in a 1D compression test corresponds to the stress, at which grain crushing occurs in the soil. The dilatational component of the frictional shear strength of dense sand decreases with

*Corresponding author, Professor, E-mail: rckwong@ucalgary.ca

increasing mean effective stress due to the fact that the amount of grains crushed increases with the applied stress at high stress levels (Bolton 1986, Yamamuro and Lade 1996). The amount of grains crushed depends on the applied stress, grain size distribution, grain shape, packing density, grain hardness and the presence or absence of water (Hardin 1985).

Although grain crushing was observed in sand under high stress compression and creep, however, no investigation has been conducted to correlate them. The objective of this paper is to compare the grain crushing mechanisms occurring in 1D compression and 1D creep tests. The first part presents a simple model quantifying the grain crushing in 1D compression using the principles of fracture mechanics and energy conservation. Then, experimental results are presented and compared to the theoretical model. Finally, similarities in the grain crushing mechanisms under 1D compression and 1D creep are explored.

2. Literature review

In the tests of Ottawa sand by Roberts and de Souza (1958), the grain size distribution curves after the 1D compression tests at different vertical stresses were obtained. Their results are shown in Fig. 1. Before the tests, the grain size in these samples ranged from 0.425 to 0.850 mm. After the tests at 7, 35, 55, and 100 MPa, the produced grains emerged in the sizes of 0.3-0.425, 0.106-0.5, 0.048-0.6, and 0.025-0.71 mm, respectively, while the grains in the sizes of 0.425-0.85, 0.5-0.85, 0.6-0.85, and 0.71-0.85 mm remained uncrushed at the corresponding vertical stresses. The term ‘produced grains’ designates the new grains created in the process of grain crushing. Fig. 1 shows that grain crushing is a progressive process in 1D compression tests of Ottawa sand.

Vallejo *et al.* (2005) conducted a series of 1D compression tests on glass beads. Typical grain size distribution curves for glass beads in their tests are shown in Fig. 2. The mass-size relation of the produced grains exhibits an approximately linear relation in the double-logarithmic plot. The linear relation indicates that the mass-size relation of the produced grains follows a fractal distribution

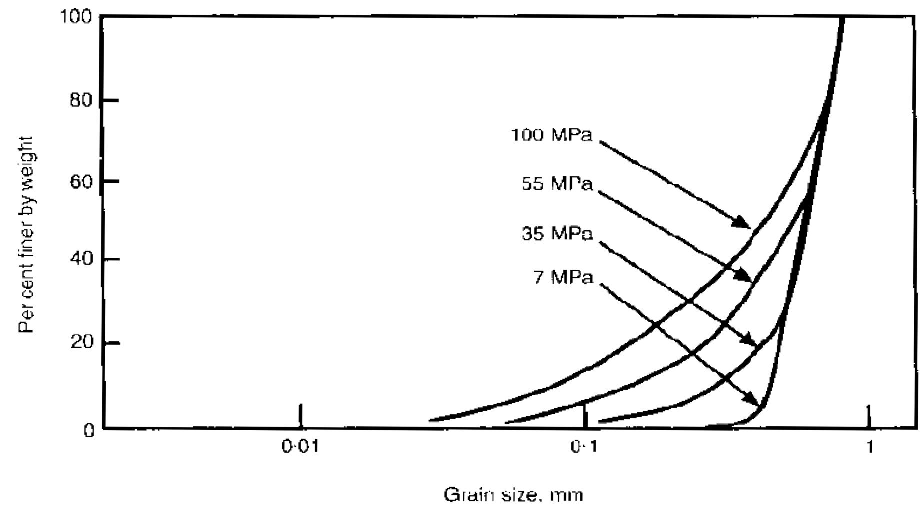

Fig. 1 Grain size evolution of Ottawa sand in 1D compression tests (Roberts and de Souza 1958)

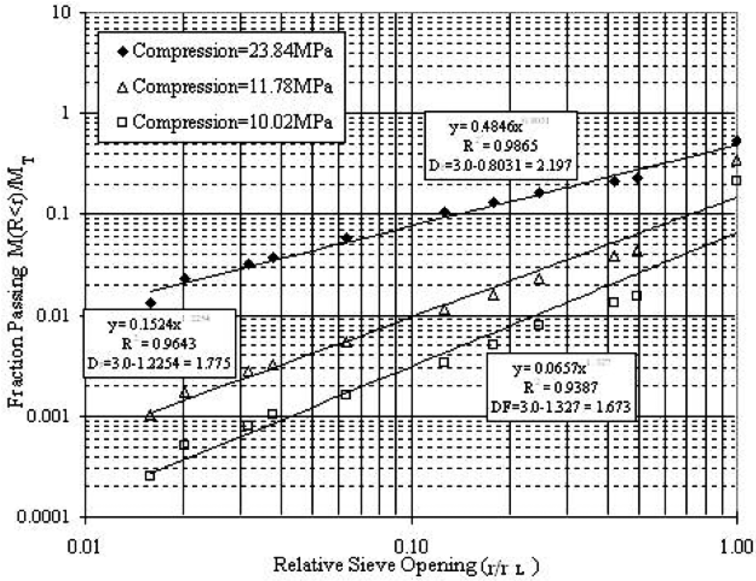

Fig. 2 Grain size evolution of glass beads in 1D compression tests (Vallejo *et al.* 2005) ($M(R<r)$ is the cumulative mass of particles with size R finer than a given comparative size r; M_T is the total mass of particles; r is the sieve size opening; r_L is the maximum particle size as defined by the largest sieve size opening used in the sieve analysis; and D_F is the fragmentation fractal dimension)

defined by a fractal dimension, D (Turcotte 1986). The fractal dimension is given as: $D=3-m$ where m is the slope of the grain size distribution. In many cases, fragmentation processes result in a fractal distribution. The fractal dimensions of the produced grains in the samples after the 1D compression tests at vertical stresses of 10.02, 11.78 and 23.84 MPa are 1.673, 1.775 and 2.193, respectively. Fig. 2 indicates that the fragmentation fractal dimension D, increases with increasing uniaxial compressive stress induced to the glass beads. The fractal dimension measures the degree of crushing of the glass beads. The greater the fractal dimension, the greater is the level of breaking of the beads. Similar trends in fractal dimensions of the produced grains in the samples were observed in the tests (Fig. 1) by Roberts and de Souza (1958). The fractal dimensions are 0.849, 1.829 and 1.856 for the tests at vertical stresses of 35, 55 and 100 MPa, respectively. McDowell and Bolton (1998) suggested that the fractal dimension is often about 2.5 for materials subjected to pure crushing, and the materials which exhibit fractal dimensions significantly different from 2.5 are usually not the products of pure crushing.

According to Mesri and Vardhanabhuti (2009), the damage of sand grains or particles could be quantified as level I damage (abrasion or grinding of grain surface), level II damage (breakage of grain corners and edges), and level III damage (fracturing, splitting, or shattering of grains) at different stress levels, respectively. For sand, level I and level II damage of sand grains occur at low stress levels and level III damage occurs at high stress levels.

Isotropic compression tests have been commonly used to investigate the cause of the creep deformation of sand. Fig. 3 shows the relations between creep strain increment and isotropic confining stress for a calcareous sand and Hostun sand (Colliat-Dangus *et al.* 1988). The increment of the creep strain is the difference in the creep strains at the elapsed time of 1 hour and 24 hours.

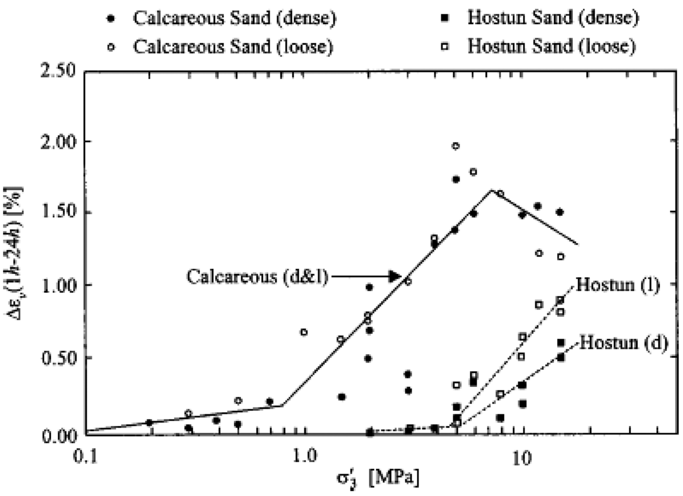

Fig. 3 Increase in volumetric creep strain between 1 and 24 h of calcareous sand and Hostun sand at different pressures in isotropic compression tests (Colliat-Dangus *et al.* 1988)

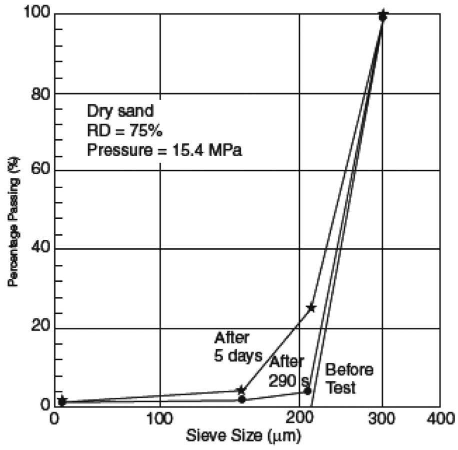

Fig. 4 Grain size distribution curves of sand samples before and after 1D creep tests (Leung *et al.* 1996)

A bilinear behavior in the creep strain increment versus confining stress relation was observed for the sandy soils. At low stress levels the creep strain increment in the same period of time increases slightly with the confining stress, while at high stress levels the increment increases significantly with the confining stress. The difference in the creep behavior at the low and high stress levels is induced by the different mechanisms of the creep deformation. At low stress levels the deformation is mostly caused by grain rearrangement, while at high stress levels the deformation is mainly caused by grain crushing. This bilinear creep behavior was also observed in the isotropic creep tests on a carbonate sand (Lagioia 1998). Bowman and Soga (2003) conducted a series of 1D creep tests on Leighton Buzzard sand and Montpellier sand at low stress levels (50 and 500 kPa). In their tests, the change in microstructure of the sands in 1D creep was investigated using the techniques of resin injection and optical microscopy of sections. It was concluded that the creep of the sandy soils at low stress levels is due to the rearrangement of the grains over time. Consistent with Bowman and Soga's observation, Kuwano and Jardine (2002) also found that in the triaxial creep tests of Ham River sand the creep deformation of the sand at low stress levels (200 and 400 kPa) is caused by the gradual stabilization of microstructures.

Leung *et al.* (1996) investigated the role of grain breakage in pile creep in sand using physical model tests. They conducted 1D creep tests on the modelled sand, and found that the amount of grains crushed increases with the duration of creep test in the 1D creep test. Fig. 4 shows the grain size distribution curves of the modelled sand before and after the 1D creep tests.

3. Energy dissipation in grain crushing

3.1 From fracture mechanics to grain crushing

The concept of fracture mechanics is used to study grain crushing in this paper. Griffith (1920) proposed two criteria for crack growth: (a) the bond at the crack tip must reach a critical value, and (b) the reduction in strain energy of the system due to the formation of a crack must be equal to or greater than the increase in surface energy required by the new crack faces.

The second criterion is known as the energy criterion for crack growth, and is expressed mathematically as (Griffith 1920)

$$\frac{\partial U_s}{\partial c} \geq \frac{\partial U_\gamma}{\partial c} \tag{1}$$

where, U_s and U_γ are the strain energy released in the system and the surface energy of the crack, respectively.

According to Griffith's energy criterion, the released strain energy is greater than the stored surface energy in the crack faces. It means that the total energy of the system, *i.e.*, the sum of the surface energy of the crack and the strain energy remaining in the system, decreases with the crack length. Meanwhile, it was found that grain crushing is always accompanied by series of acoustic emissions events (Karner *et al.* 2003, Graham *et al.* 2004). Thus, the total energy dissipated in the process of fracturing or grain crushing is greater than the surface energy stored in the newly created surfaces.

This study assumes that the released strain energy is expended in the surface energy of created fracture faces during fracturing. A new quantity, termed the specific fracture energy, γ is introduced in this study. It is defined as the amount of released strain energy per unit surface area of the crack, *i.e.*, dividing the released strain energy U_s in Eq. (1) by the surface crack area, A_c.

It is of importance to note that this study assumes that the released strain energy is proportional to the surface energy of the newly created surfaces, although they are not equal, because part of the total energy is dissipated in acoustic emissions.

3.2 Specific fracture energy for Hertzian fracture

In modelling the discrete nature of granular soil, the Hertz contact is widely used to describe the interactions among the grains in granular soil (Fig. 5). The relation between the radius of the contact and the force applied on the indenter may be expressed as (Hertz 1896)

$$a^3=\frac{3}{2}\frac{PR}{E}(1-\nu^2) \tag{2}$$

where a is the radius of the contact; P is the indenter force; R is the radius of the spherical indenter; E and υ are the Young's modulus and Poisson's ratio for the indenter and flat surface materials. Hertz (1896) found that the maximum tensile stress occurs at the edge of the contact circle and may be given as

$$\sigma_{max}=\frac{P}{2\pi a^2}(1-2\nu) \tag{3}$$

When the above radial tensile stress reaches a critical value, a conical crack, termed a Hertzian fracture, is developed in the solid as shown in Fig. 5.

In the case of two identical spherical grains in contact, the crack starts to initiate at a point of radius r_0 as shown in Fig. 5. The value of r_0/a may be assumed to be unity (Fischer-Cripps 1997). With analogy to the case of Griffith's crack growth, the specific fracture energy for Hertzian

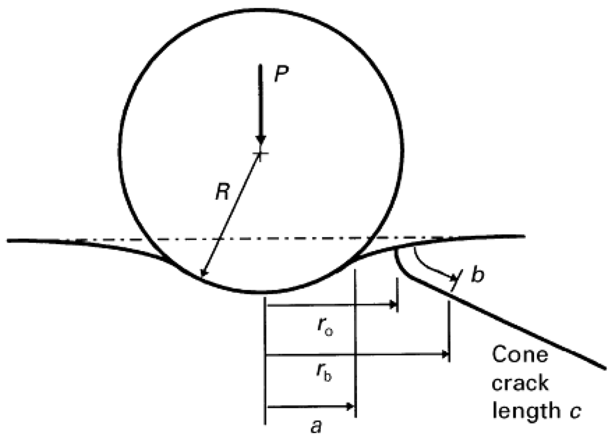

Fig. 5 Hertzian contact and Hertzian fracture. a is radius of the contact, c is crack length, r_0 is radius of the starting point of the crack, b is variable on the travel of the crack with radius of r_b (Fischer-Cripps 1997)

fracture, *i.e.*, fracture energy per unit volume of soil, may be expressed as

$$\gamma_H = \frac{2\sigma_v R}{3\pi^2 Y_H^2} \Psi_{r_0/a=1} \tag{4}$$

where σ_v is the applied vertical stress across the grain diameter ($P=\pi R^2\sigma_v$); $\Psi_{r_0/a=1}$ is the value of the integral function at $r_0/a=1$ and may be considered as a constant (this integral function is characteristic of the pre-existing stress field); Y_H is the geometry shape factor of Hertzian fracture; and R is the radius of the spherical grain. Eq. (4) indicates that the specific fracture energy for a Hertzian fracture in the sphere-to-sphere contact depends on the material properties, the applied stress and the radius of the spherical grain.

3.3 Fracture surface area in grain crushing in 1D compression

When a sand sample is subjected to 1D compression, sand grains are crushed and the surface area of grains increases with the amount of grains crushed. The increase in surface area in crushed grains should be twice as much as the total area of fracture surface of the crushed grains in the sample. The fracture surface area could be obtained using the mode of grain size evolution in 1D compression (Wang 2010). He found that the specific fracture surface area, a_c, *i.e.*, fracture surface per unit volume of soil could be assumed proportional to the amount of grains crushed

$$a_c = \alpha \frac{\varphi_c}{\sqrt{d_1 d_2}} \tag{5}$$

where φ_c is defined as the relative amount or the ratio of the volume of grains crushed divided by the total volume of grains; α is a proportionality constant; and d_1 and d_1 are the smallest and largest crushed grain sizes, respectively. Thus, the specific energy expended in grain crushing is equal to the product of the specific fracture energy, γ_H and the specific fracture surface area, a_c.

3.4 Energy equation in 1D compression with grain crushing

In the 1D compression of granular soil, grain fracturing occurs extensively in the soil. The grains produced in the first several processes of fracturing may be crushed again when the soil is subjected to an increased stress in compression. In addition, the sizes of grains are different, and different contact forces are exerted on each grain. These complex factors make the study of the influence of grain crushing on the deformation of granular material to a challenging problem.

To overcome this complexity, the energy method has been used (Miura and O-Hara 1979, Ueng and Chen 2000, McDowell and Bolton 1998). The energy dissipated in grain crushing was included in the Cam-Clay work equation (Roscoe *et al.* 1963, Schofield and Wroth 1968)

$$q\varepsilon_q^p + p'\varepsilon_v^p = Mp'\varepsilon_q^p + u_c \tag{6}$$

where q and p' are the deviatoric and mean effective stresses, respectively; ε_q^p and ε_v^p are the deviatoric and volumetric plastic strains, respectively; M is a constant relating to the friction angle at critical state, which is given by $M = 6\sin\phi_c/(3-\sin\phi_c)$; and ϕ_c is the friction angle at critical state. The first and second terms on the left-hand side of Eq. (6) represent the work per unit volume of soil done by the deviatoric and mean effective stresses, respectively. The first term on the right-hand side is the energy per unit volume of soil dissipated in friction. The second term u_c is the energy per unit volume of soil dissipated in the process of grain crushing, quantified as the specific surface energy, which is stored in the newly created surface.

As mentioned above, the total energy dissipated in the process of grain crushing could be estimated with the strain energy released in the soil, which is related to the specific fracture surface area. The specific energy dissipated in the process of grain crushing may be obtained using Eqs. (4) and (5).

In order to extend the concept of specific fracture energy dissipated in grain crushing, another modification was made to Eq. (4) relating to the typical size of the system. In the case of Hertzian fracture, the sphere radius is used to normalize the crack length. In the case of granular soil, the sizes of the grains in sand are different. Therefore, a characteristic size should be chosen as the typical size of grains. Recall that in the expression for specific surface area of the produced grains in 1D compression, *i.e.*, Eq. (5), a typical grain size $\sqrt{d_1 d_2}$ is used. This typical size might be a good choice in representing the variation in grain sizes in the soil.

In 1D condition, the ratio of the horizontal effective stress σ_h', over the vertical effective stress σ_v', of the soil is given with Jaky's semi-empirical formula as (Jaky 1944)

$$K_0 = \frac{\sigma_h'}{\sigma_v'} = 1 - \sin\phi \tag{7}$$

where ϕ is the friction angle of the soil. With Jaky's formula, the stress invariants in the energy Eq. (6) in 1D condition can be written as

$$q = \sigma_1 - \sigma_3 = \sigma_1 \sin\phi \tag{8}$$

$$p' = \frac{1}{3}(\sigma_1 + 2\sigma_3) = \frac{(3 - 2\sin\phi)}{3}\sigma_1 \tag{9}$$

where σ_1 and σ_3 are the major (axial) and minor (radial) stresses, respectively.

The strain invariants are expressed as

$$\varepsilon_q^p = \frac{2}{3}(\varepsilon_1^p - \varepsilon_3^p) \tag{10}$$

$$\varepsilon_v^p = \varepsilon_1^p + 2\varepsilon_3^p \tag{11}$$

where $\varepsilon_3^p = 0$ in the 1D case.

With these invariants, Eq. (6) becomes

$$\varepsilon_v^p = \frac{1}{\mu}\frac{u_c}{\sigma} \tag{12}$$

where

$$\mu = 1 - \frac{2(1+2K_0)M}{9};\ u_c = a_c\gamma_H$$

As the friction angle of the soil does not change significantly, μ could be considered as a material constant. As $\varepsilon_v^p = (e - e_0)/(1+e_0)$, Eq. (12) is rewritten as

$$e = e_0 - C_p\varphi_c \tag{13}$$

in which e_0 is the void ratio at the yield stress of the soil, and C_p is the coefficient of the relation between the void ratio and grain crushing amount of the soil, called the plastic crushability index, which becomes

$$C_p = \frac{2\alpha\Psi_{r_0/a=1}}{3\mu\pi^2 Y_H^2} \tag{14}$$

From Eq. (13), it can be found that in 1D compression of granular soil, the void ratio is proportional to the grain crushing amount. That is, the extent of the deformation of granular soil at high stresses is proportional to the amount of grains crushed. It is of importance to understand that Eq. (13) derived based on the fundamentals of fracture mechanics and energy conservation law could be reduced to a simple linear function because several idealized assumptions are made in the derivation.

4. Test material, setup and program

The material used in the tests is unground ASTM 20/30 silica sand, which was mined at Ottawa, Illinois in USA. In the grain solid, the content of silicon dioxide is about 99.8%. The sand has a specific gravity of 2.65. The batch of grains with the size in the range of 0.595 to 0.841 mm was used to prepare samples.

The 1D compression and creep tests were conducted using an oedometer cell (Fig. 6). The apparatus consists of a steel confining ring, a steel pedestal, two steel compression plates, a loading guide and a piston. The confining ring has a diameter of 6.35 cm and a height of 2.54 cm. The vertical force was applied using a loading system, Material Test System® (MTS), with a capacity of 100 kN. It can be operated under load or displacement controlled mode. An external laser

Fig. 6 Compression apparatus for 1D compression and 1D creep tests of Ottawa sand

displacement transducer (Keyence) was used to measure the displacement of sand samples The resolution is ±0.001 mm.

The sand samples were prepared using the air pluvial method. The initial void ratio of the samples is about 0.543. A loading rate of 10 kN/min was used in the 1D compression tests. After each 1D compression or creep test, the sample was collected for grain size analysis. The grain size analysis was conducted using a stack of sieves consisting of opening sizes No. 30, 35, 45, and 60 (0.595, 0.500, 0.354 and 0.250 mm), respectively. A scale of high accuracy (±0.001 g) was used to measure the mass of grains from each sieve. The 1D creep tests on Ottawa sand were conducted at three stress levels: 10, 18, and 28 MPa. The durations of tests at each stress level were 15, 30, 60 and 120 minutes.

5. Test results and discussion

5.1 1D Compression tests

Fig. 7 shows the compression curve of Ottawa sand. The sand displays a nonlinear relation between the void ratio and confining stress. The relation could be approximated by two compression indices, 0.006 and 0.05 for stress ranges of 0.1 to 10 and 10 to 28 MPa, respectively.

Fig. 8 shows the relation between the grain crushing amount and compression stress. The grain crushing amount was calculated using the measure proposed by Leslie (1963), *i.e*., the ratio of the mass of the grains passing the smallest sieve No. 30 (0.595 mm) used in the experiment over the total mass of the whole sample. In the regime of low stress (less than 10 MPa), the grain crushing amount is quite low or non-detectable, while in the regime of high stress, the grain crushing amount is high and increases with the vertical stress. The transition of the two regimes occurs at about 10 MPa.

Fig. 9 shows the grain size distribution curves of the sand under the vertical stresses of 10, 18 and 28 MPa. The grain crushing amount increases with vertical stress. Fig. 10 shows the void ratio versus grain crushing amount relation. Fitting the data with Eq. (13), it gives e_0=0.529 and

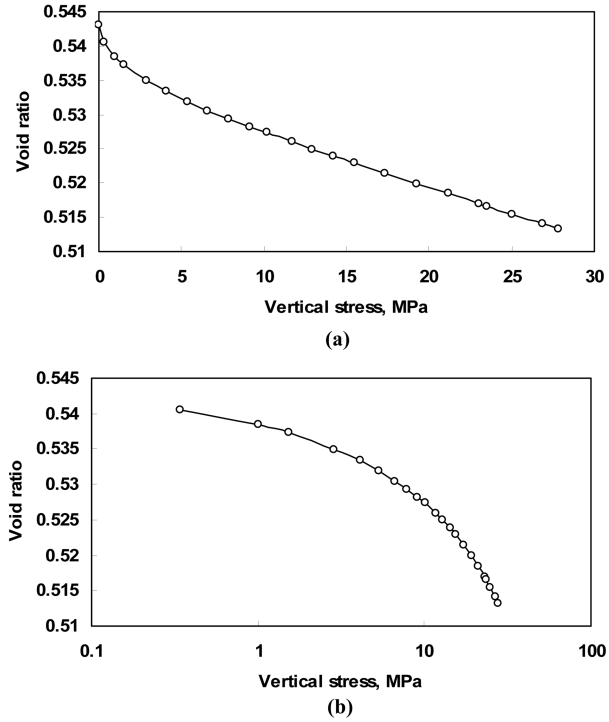

Fig. 7 1D compression curves of Ottawa sand: (a) void ratio versus vertical stress relation and (b) void ratio versus logarithm of vertical stress relation

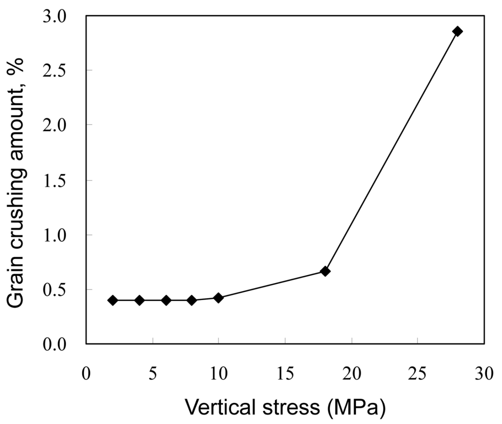

Fig. 8 Relation between grain crushing amount and compression stress in 1D compression tests of Ottawa sand

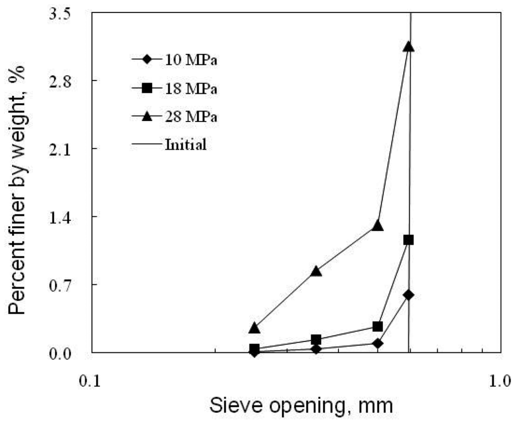

Fig. 9 Grain size distribution curves of Ottawa sand after 1D compression tests at different vertical stresses

C_p=0.50. Data of grain crushing at stresses less than 10 MPa are not included in Fig. 10. At these stress levels, the grain damage is induced by abrasion of grain surface and breakage of grain corners and edges (levels I and II as proposed by Mesri and Vardhanabhuti (2009)), rather than fracturing (level III).

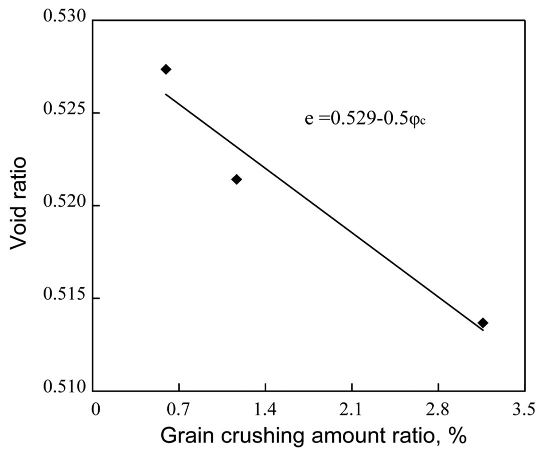

Fig. 10 Relation between void ratio and grain crushing amount in 1D compression tests of Ottawa sand

Table 1. 1D compression test data of granular materials related to grain crushing

Label	Reference	Material	Grain shape	Grain sizes (mm)	Initial void ratio	Stress range (MPa)	C_p	Yielding stress (MPa)	C_c	Void ratio at yielding	
										Eq. (14)	Casagrande's method
OS1	Roberts & de Souza 1958	Ottawa sand	Round	0.425-0.85	0.60	7-100	0.54	29	0.47	0.60	0.55
OS2	Hagerty *et al.* 1993	Ottawa sand	Round	0.425-0.85	0.70	21-689	0.79	20	0.35	0.63	0.61
BBS	Hagerty *et al.* 1993	Slag	Angular	0.425-0.85	0.80	21-689	0.61	10	0.37	0.79	0.69
PC	Bard 1993	Petroleum coke	Angular	5-10	2.30	5-100	1.72	0.5	1.15	2.02	2.1
SS1	Nakata *et al.* 2001	Silica sand	Angular	1.4-1.7	0.63	1.7-92	0.43	20	0.49	0.62	0.54
SS2	Nakata *et al.* 2001	Silica sand	Angular	0.25-2.0	0.60	3.6-92	1.14	30	0.48	0.61	0.48
PS	McDowell & Khan 2003	Pasta	Flaky	6.25-15	2.40	0.4-1	1.25	0.08	1.45	1.63	2.2
OS3	This study	Ottawa sand	Round	0.591-0.85	0.543	10-28	0.50	10	0.05	0.53	0.53

Note: C_c is the compression index after yielding

The 1D compression test data of granular materials in the literature were collected and examined. The published test data are tabulated in Table 1, along with the test data of sand from this study. The materials in the table cover from highly crushable petroleum coke and pasta to quartz sands. In the table, the grain shape, initial grain sizes and the initial void ratio are included. Plastic crushability index and void ratio at yielding of the material were estimated from Eq. (13) for each

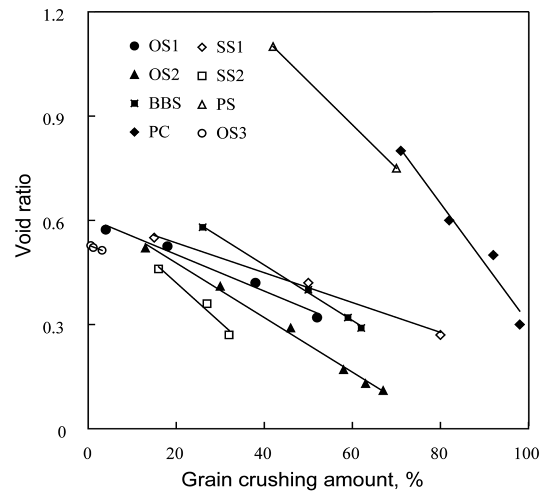

Fig. 11 Void ratio-grain crushing amount relation of granular materials in 1D compression tests (Labels refer to Table 1)

material. Fig. 11 compares the test data with the predictions from Eq. (13). The prediction is consistent with the test data, *i.e.*, the void ratio decreases linearly with increasing grain crushing amount. To be consistent, the grain crushing amounts were estimated using the same measure proposed by Leslie (1963). Other measures of particle breakage (Hardin 1985) could be used in the analysis, but they yield relative factors rather than absolute values. Since Eqs. (5) and (13) are formulated in terms of the volume of grains crushed, thus the measure proposed by Leslie (1963) is used in the study.

The yield points of different materials listed Table 1 were estimated using Casagrande's method (Casagrande 1936), in which the yield point corresponds to the maximum curvature point of the void ratio-log vertical stress curve. The estimated void ratios at yielding of Ottawa sand by Hagerty *et al.* (OS2) and petroleum coke (PC) are close to those predicted from Eq. (13) by setting φ_c=0. However, the estimated void ratios at yielding of other materials using Casagrande's method are lower than those predicted by Eq. (13). From Table 1, it is evident that the plastic crushability index of granular material is influenced by the physical properties and grading of the material. The plastic crushability indices of petroleum coke and pasta are higher than those of sands, and the crushability index of well graded silica sand (SS2) is higher than that of uniform silica sand (SS1).

5.2 1D creep tests

Fig. 12 shows the creep curves of Ottawa sand subjected to different vertical stresses. The creep rate of Ottawa sand decreases with time, but increases with vertical stress. Test data of each test series should yield an overlapping pattern. The inconsistent creep behaviour observed in the 10-MPa test series might be due to the sample heterogeneity. In terms of axial strain, the average creep rates in the first 30 minutes are about 6.3×10^{-5}, 9.3×10^{-5} and 9.3×10^{-4} %/minute in the tests at 10, 18 and 28 MPa, respectively. These observed creep rates are much higher than those observed in sandstones samples by (Li and Xia 2000) which are in a range of 2.5×10^{-8} to 5.0×10^{-9} %/minute.

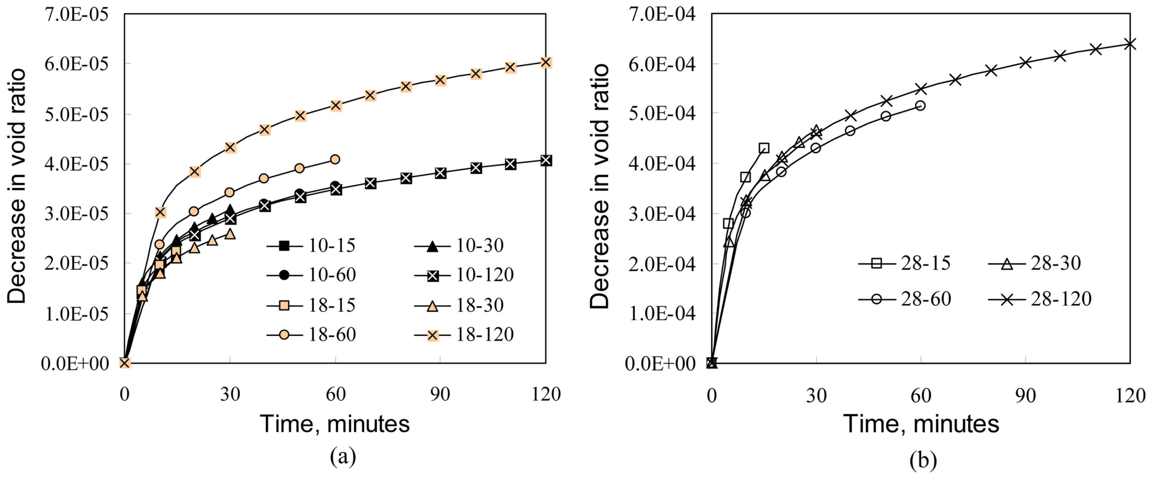

Fig. 12 1-D Creep curves of Ottawa san at vertical stresses of (a) 10 and 18 MPa and (b) 28 MPa (Legend 10-15 denotes the creep test at 10 MPa for 15 minutes)

This comparison indicates that the creep deformation observed in this study is mainly due to the grain crushing, rather than the creep in solid grains themselves.

Fig. 13 shows the grain size distribution curves for samples at different vertical stresses. It was found that the grain size distribution curves after 1D creep tests are similar to those after 1D compression tests. Fig. 14 compares the grain size distribution curves with the typical fractal number-size relation. The fractal dimension increases with increasing grain crushing amount. It is postulated that at low stress level (<10 MPa) most damage of grains in the sand samples is on the levels I (abrasion or grinding of grain surface) and II (breakage of grain corners and edges), while at high stress (≥10 MPa) damage of grains is on the level III (fracturing, splitting, or shattering of

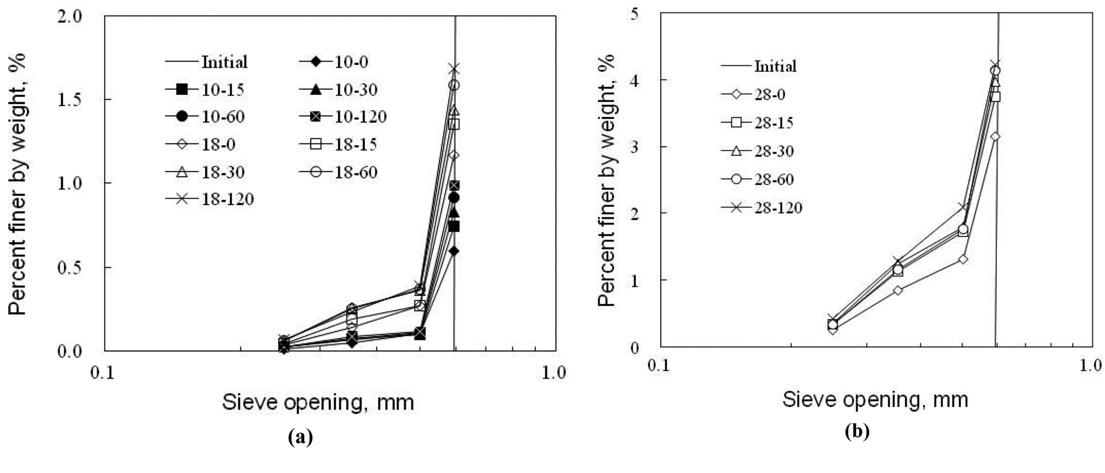

Fig. 13 Grain size distribution curves of Ottawa sand in 1D compression and creep tests for different periods of elapsed time at vertical stresses of (a) 10 and 18 MPa and (b) 28 MPa (Legend 10-15 denotes the grain size distribution curve of the sample after the creep test at 10 MPa for 15 minutes)

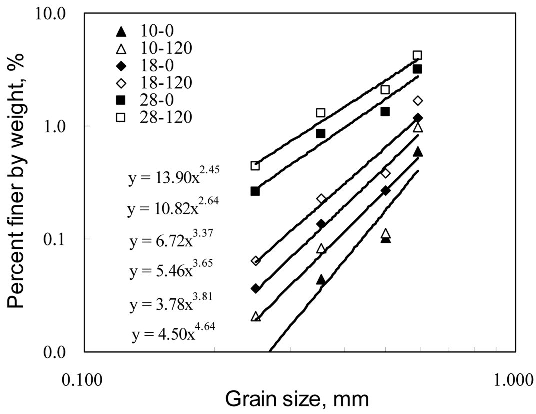

Fig. 14 Variation of fractal dimension in 1D compression and creep tests on Ottawa sand

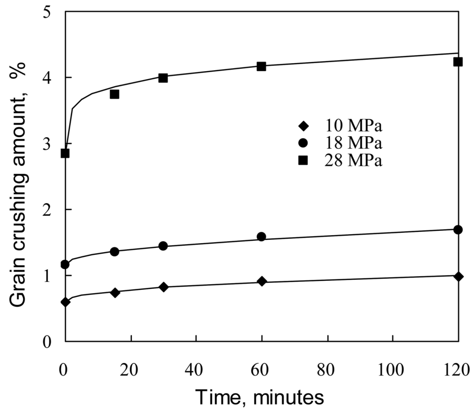

Fig. 15 Relations between grain crushing amount and time in 1D creep tests on Ottawa sand at different vertical stresses, along with fittings from Eq. (17)

grains). It is believed that the fractal mass-size distribution only holds for the grains subject to the splitting of grains (McDowell *et al.* 1996).

Fig. 15 shows the relations between grain crushing amount and time in the creep tests, noting that the initial grain crushing amounts were obtained in the 1D compression tests. The grain crushing amount increases with both time and vertical stress. To investigate the relation between the creep rate in terms of void ratio and grain crushing rate of Ottawa sand in the 1D creep tests, void ratio versus time and grain crushing amount versus time relations were fitted with power functions, which are expressed as

$$e=e_i+a_e t^{m_e} \tag{15}$$

$$\varphi_c=\varphi_{ci}+a_\varphi t^{m_\varphi} \tag{16}$$

where, e_i is the initial void ratio; a_e and m_e are the parameters for void ratio-time relation; φ_i is the initial grain crushing amount; a_φ and m_φ are the parameters for grain crushing amount-time relation. The parameters for the relations are presented in Table 2. The relation between the creep rate in terms of void ratio and grain crushing rate was obtained from Eqs. (15) and (16)

$$\dot{e}=\frac{a_e m_e}{a_\varphi m_\varphi} t^{m_e-m_\varphi} \dot{\varphi}_c \tag{17}$$

Table 2. Parameters for void ratio-time and grain crushing amount-time relations of Ottawa sand

Vertical stress (MPa)	a_e	m_e	a_φ	m_φ
10	-1.2×10^{-4}	0.26	5.3×10^{-4}	0.43
18	-1.8×10^{-4}	0.26	5.8×10^{-4}	0.46
28	-1.9×10^{-4}	0.26	5.6×10^{-3}	0.20

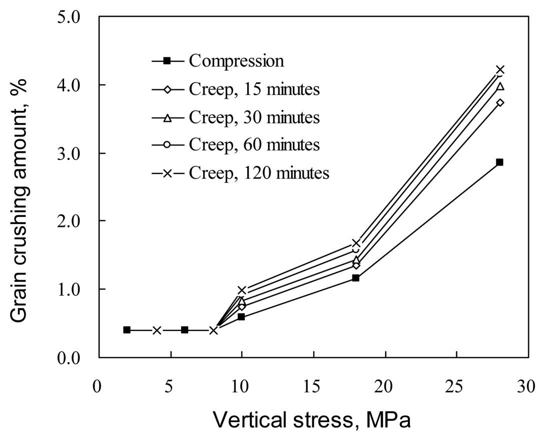

Fig. 16 Relations between grain crushing amount and vertical stress in 1D compression and creep tests on Ottawa sand

Eq. (17) relates the creep rate (on macroscopic scale) to the change rate of grain size distribution (on microscopic scale) in Ottawa sand when it is subjected to 1D creep. For $m_c \approx m_\varphi$, the relation between the creep rate and grain crushing rate becomes linear, and the viscous crushability index (C_{vs}) can be estimated as

$$C_{vs} = \frac{a_e m_e}{a_\varphi m_\varphi} \tag{18}$$

According to the parameters in Table 2, the viscous crushability index of Ottawa sand is within the range of 0.05-0.12 in the creep tests.

Fig. 16 shows the relations between grain crushing amount and vertical stress in the 1D compression and creep tests. The bilinear relation between the grain crushing amount and vertical stress in the compression behaviour was also found in the creep behaviour of Ottawa sand. In the regime of low stresses (<10 MPa), the grain crushing amount rate is small or non-detectable, while in the regime of high stresses (≥10 MPa), the grain crushing amount rate increases with both the vertical stress and time. In the creep tests, it was observed that the creep rate and grain crushing rate change significantly beyond the yield stress. Therefore, the yield stress of granular soil marks the abrupt onset of the increase in the amount of damaged grains on level III, as suggested by Mesri and Vardhanabhuti (2009).

At high stresses (≥10 MPa), the grain crushing amount increases with both the vertical stress and time. Thus, it is expected that, for any time in a creep test, there is a corresponding vertical stress, at which the grain crushing amount is the same as that in the creep test at that time. That is, the effects of time and vertical stress are equivalent in changing the soil fabric from one state to the other state, characterized with the same grain size distribution. Therefore, the equivalent effect substantiates the same potential of plastic and creep flow rules proposed by Lade and Liu (1998). It is important to note that the equivalent effect is only valid for the test materials and testing conditions used in this study.

6. Conclusions

The effect of grain crushing on the deformation of sand in 1D compression and 1D creep at high stresses was studied. A theoretical approach was proposed to formulate the process of grain crushing in accordance with the laws of fracture mechanics and energy conservation. In this approach, the concept of specific fracture energy was extended from the simple Hertzian fracture problem to the complex circumstance of grain crushing. With some idealized assumptions, a simple linear relationship between the void ratio and the grain crushing amount of soil in 1D compression was derived. Experimental data were used to verify this linear function. In 1D creep tests, it was observed that the creep rate is a function of the void ratio and the grain crushing rate. The evolution of grain size distributions observed in the 1D compression tests is comparable to that observed in 1D creep tests. The equivalent effects of stress and time on the grain crushing process are drawn, *i.e.*, both the stress and time exert equivalent effect in grain crushing or change in the soil fabric. This indicates that the potentials for plastic and creep flows may be the same under 1D compression and 1D creep conditions.

Acknowledgements

This study was made possible with financial supports from Natural Sciences and Engineering Research Council of Canada and Department of Civil Engineering, The University of Calgary.

References

Bard, E. (1993), "Comortement des matériaux granulaires secs et à liant hydrocarbone", PhD thesis, Ecole Centrale de Paris.

Bolton, M.D. (1986), "The strength and dilatancy of sands", *Geotech.*, **36**(1), 65-78.

Bowman, E.T. and Soga, K. (2003), "Creep, ageing and microstructural change in dense granular materials", *Soils Found.*, **43**(4), 107-117.

Casagrande, A. (1936), "Determination of the preconsolidation load and its practical significance", *Proceedings of International Conference on Soil Mechanics and Foundation Engineering*, **3**, 60-64.

Colliat-Dangus, J.L., Desrues, J. and Foray, P. (1988), *Triaxial testing of granular soil under elevated cell pressure*, Advanced triaxial testing of soil and rock, ASTM, edited by Donaghe *et al.*, Philadelphia, 290-310.

Coop, M.R. (1990), "The mechanics of uncemented carbonate sands", *Geotech.*, **40**(4), 607-626.

Fischer-Cripps, A.C. (1997), "Predicting Hertzian fracture", *J. Mater. Sci.*, **32**(5), 1277-1285.

Graham, J., Alfaro, M. and Ferris, G. (2004), "Compression and strength of dense sand at high pressures and elevated temperatures", *Can. Geotech. J.*, **41**(6), 1206-1212.

Griffith, A.A. (1920), *The phenomena of rupture and flow in solids*, Philosophical Transactions of the Royal Society of London, Serial B, **221**, 163-198.

Hagerty, M.M., Hite, D.R., Ullrich, C.R. and Hagerty, D.J. (1993), "One-dimensional compression of granular media", *J. Geotech. Eng.*, **119**(1), 1-18.

Hardin, B.O. (1985), "Crushing of soil particles", *J. Geotech. Geoenviron. Eng.*, **111**(10), 1177-1192.

Hertz, H. (1896), *On the contact of elastic solids*, In Jones & Schott (Eds.) miscellaneous paper, London, Macmillina.

Jaky, J. (1944), "The coefficient of earth pressure at rest", *J. Soc. Hungarian Architect. Eng.*, 355-358.

Karner, S.L., Chester, F.M., Kronenberg, A.K. and Chester, J.S. (2003), "Subcritical compaction and yielding of granular quartz sand", *Tectonophysics*, **377**(3-4), 357-381.

Kuwano, R. and Jardine, R.J. (2002), "On measuring creep behavior behaviour in granular materials through triaxial testing", *Can. Geotech. J.*, **39**(5), 1061-1074.

Lade, P.V. and Liu, C.T. (1998), "Experimental study of drained creep behavior of sand", *J. Eng. Mech.*, **124**(8), 912-920.

Lade, P.V., Yamamuro, J.A. and Bopp, P.A. (1996), "Significance of particle crushing in granular materials", *J. Geotech. Eng.*, **122**(4), 309-316.

Lagioia, R. (1998), "Creep and apparent preconsolidation in carbonate soils", The geotechnics of hard soil-soft rocks, edited by Evangelista, A. and Picarelli, L., Balkema, Rotterdam, The Netherlands.

Leslie, D.D. (1963), "Large scale triaxial tests on gravelly soils", *Proceedings of the 2nd Panamerican Conference on Soil Mechanics and Foundation Engineering*, Brazil, **1**, 181-202.

Leung, C.F., Lee, F.H. and Yet, N.S. (1996), "The role of particle breakage in pile creep in sand", *Can. Geotech. J.*, **33**(6), 888-898.

Li, Y. and Xia, C. (2000), "Time-dependent tests on intact rocks in uniaxial compression", *Int. J. Rock Mech. Min.*, **37**(3), 467-475.

McDowell, G.R. and Bolton, M.D. (1998), "On the micromechanics of crushable aggregates", *Geotech.,* **48**(5), 667-679.

McDowell, G.R., Bolton, M.D. and Robertson, D. (1996), "The fractal crushing of granular materials", *J. Mech. Phys. Solids*, **44**(12), 2079-2102.

McDowell, G.R. and Khan, J.J. (2003), "Creep of Granular materials", *Granul. Matter*, **5**(3), 115-120.

Mesri, G. and Vardhanabhuti, B. (2009), "Compression of granular materials", *Can. Geotech. J.*, **46**(4), 369-392.

Mitchell, J.K. and Soga, K. (2005), *Fundamentals of soil behaviour*, 3rd ed., John Wiley & Sons, New Jersey.

Miura, N. and O-Hara, S. (1979), "Particle-crushing of a decomposed granite soil under shear stresses", *Soils Found.*, **19**(3), 1-14.

Nakata, Y., Kato, Y., Hyodo, M., Hyde, A.F.L. and Murata, H. (2001), "One-dimensional compression behavior of uniformly graded sand related to single particle crushing strength", *Soils Found.*, **41**(2), 39-51.

Nakata, Y., Kato, Y., Hyodo, M., Murata, H. and Harada, T. (1999), "Particle crushing of granular materials subjected to one dimensional compression", *Proceedings of Symposium on Engineering problem on crushable ground*, 15-20.

Roberts, J.E. and de Souza, J.M. (1958), "The compressibility of sands", *Proceedings of American Society of Testing and Materials*, **58**, 1269-1277.

Roscoe, K.H., Schofield, A.N. and Thurairajah, A. (1963), "Yielding of clays in states wetter than critical", *Geotechnique*, **13**(3), 211-240.

Schofield, A.N. and Wroth, C.P. (1968), *Critical state soil mechanics*, McGraw-Hill, London.

Turcotte, D.L. (1986), "Fractal and fragmentation", *J. Geophys. Res.*, **91**(B2), 1921-1926.

Ueng, T.S. and Chen, T.J. (2000), "Energy aspects of particle breakage in drained shear of sands", *Geotechnique*, **50**(1), 65-72.

Vallejo, L.E., Lobo-Guerrero, S. and Chik, Z. (2005), *A network of fractal force chains and their effect in granular materials under compression*, In Fractals in engineering: New trends in theory and applications 2, 67-80.

Wang, Z. (2010), "Soil creep behavior-laboratory testing and numerical modelling", PhD thesis, Department of Civil Engineering, University of Calgary.

Wood, D.M. (2007), "The magic of sands- the 20th Bjerrum Lecture presented in Oslo", *Can. Geotech. J.*, **44**(11), 1329-1350.

Yamamuro, J.A. and Lade, P.V. (1996), "Drained sand behavior in axisymmetric tests at high pressures", *J. Geotech. Eng.*, **122**(2), 109-119.

PL